

Millimeter-VLBI with a Large Millimeter-Array: Future Possibilities

Thomas P. Krichbaum

Max-Planck-Institut für Radioastronomie, Auf dem Hügel 69, D-53121 Bonn,
Germany

appeared in: 'Science with Large Millimeter Arrays', ESO Astrophysical Symposia, ed. P.A. Shaver, Springer (Berlin Heidelberg), 1996, p. 95-102 (ISBN 3-540-61582-2).

Millimeter-VLBI with a Large Millimeter-Array: Future Possibilities

Thomas P. Krichbaum

Max-Planck-Institut für Radioastronomie, Auf dem Hügel 69, D-53121 Bonn, Germany

Abstract. We discuss possibilities and improvements which could be obtained, if a phased array with a large number ($N = 50 - 100$) of sub-millimeter antennas – like the planned large southern array (LSA) – is used for radio-interferometry with very long baselines (VLBI) at millimeter wavelengths. We find that the addition of such an instrument will push the detection limit and the imaging capabilities of a global mm-VLB-interferometer by 1-2 orders of magnitude.

1 Introduction

The Very Long Baseline Interferometry (VLBI-) technique (eg. Thompson, Moran & Swenson, 1986; Zensus, Diamond & Napier, 1995) is used to study compact radio sources. The classes of objects which can be studied at centimeter wavelengths range from the ultra-luminous nuclei of radio-loud quasars, blazars and BL Lac-objects and their emanating jets, to the moderately luminous radio-galaxies, Seyfert- and starburst galaxies. With milli-Jansky sensitivity at centimeter-wavelengths, also the mapping of peculiar binary stars (eg. Cyg X-3, SS 433), radio-stars and young supernova remnants (eg. SN 1993J) now is possible. Spectroscopic VLBI-observations allow to investigate compact maser emitting regions of various kinds (eg. OH-, CH₃OH, H₂O, SiO) in galaxies, star birth regions and stellar envelopes. Polarization-VLBI observations show the polarized structure of compact radio sources on milli-arcsecond scales. The phase-referencing technique allows to determine source positions with highest possible accuracy. In geodesy, VLBI is used to derive earth-rotation parameters and to measure the motion of tectonic plates.

At millimeter wavelengths ($\lambda \leq 0.7$ mm, $\nu \geq 43$ GHz) present VLBI-observations allow imaging with an angular resolution of up to $40 \mu\text{as}$ ($1 \mu\text{as} \hat{=} 10^{-6}$ arcsec) at 3 mm wavelength (eg. Bååth *et al.*, 1992). This gives the opportunity to study physical processes in regions of micro-arcsecond size, corresponding to a few up to a few hundred lightdays in a source at cosmological distance $z \geq 0.01$.

To date mm-VLBI is done mostly with telescopes designed for observations at longer wavelengths. This and the limitations set by not yet fully optimized receivers (T_{sys} in the range of 200 – 1000 K at 86 GHz), still limit the detection sensitivity to about 0.2 – 0.5 Jy in recent 3 mm-VLBI observations (eg. Standke *et al.*, 1994, Schalinski *et al.*, 1994). The addition of sub-millimeter telescopes

(eg. the IRAM 30 m telescope on Pico Veleta, Spain) has helped considerably to push the detection thresholds below the 1 Jy level (eg. Krichbaum *et al.*, 1993 & 1994), but antenna apertures of typically 10^4 m^2 are needed to reach the milli-Jansky (mJy-) level, which now is accessible at the longer cm-wavelengths without major efforts.

2 Why millimeter-VLBI ?

Opacity: Most compact extragalactic radio sources are partially self-absorbed at cm-wavelengths. For a given brightness temperature T_B and flux density S of the radio source, the size θ of the emitting region only depends on the observing wavelength λ :

$$\theta \propto \lambda \cdot \sqrt{\frac{S}{T_B}} \quad (1)$$

Millimeter-VLBI observations therefore provide twofold advantage: high angular resolution and imaging of small scale regions, which are self-absorbed at longer wavelengths and which cannot be studied directly by other methods.

Recently the frequency band accessible for mm-VLBI was extended to $\lambda = 1.4 \text{ mm}$ ($\nu = 215 \text{ GHz}$) (Greve *et al.*, 1995). This and earlier studies with US-american instruments at 223 GHz (Padin *et al.*, 1990) and at 86 GHz (Rogers *et al.*, 1984) indicate that the sources are sufficiently bright and compact and that the limitations set by the atmosphere (coherence) still allow VLBI observations up to frequencies of at least 300 GHz.

Assuming brightness temperatures below the inverse Compton-limit ($T_B \leq 10^{12} \text{ K}$) equation (1) yields a minimum size for a source of flux density S (in [Jy]) of $\theta > (1.22 \cdot S \cdot \nu^{-2})^{1/2} = 4 \cdot \sqrt{S} \mu\text{as}$ at $\nu = 300 \text{ GHz}$. The rapid flux density variations of the ‘intraday variable’ (IDV-) compact radio sources suggest that the variable component in this class of objects is even more compact (eg. Wagner & Witzel, 1995). This has the important consequence that at millimeter wavelengths objects with the highest brightness temperatures will still appear unresolved on interferometer baseline lengths of $< 20\,000 \text{ km}$. Less compact radio sources, however, with more typical brightness temperatures in the range of $T_B = 10^9\text{--}10^{11} \text{ K}$ will be partially resolved by the interferometer beam. It is therefore possible to study their underlying structure with unprecedented accuracy.

Angular and spatial resolution: The angular resolution A of a radio interferometer is proportional to the observing wavelength λ and inversely proportional to the relative separation or baseline b between two antennas:

$$A \propto \frac{\lambda}{b}, \text{ or in convenient units: } A_{[\text{mas}]} = 3.1 \cdot 10^4 \cdot \frac{1}{\nu_{[\text{GHz}]} \cdot b_{[\text{km}]}} \quad (2)$$

Since b is limited by the earth’s diameter, the only way to achieve higher angular resolution is to go to shorter wavelengths ($\lambda \rightarrow \text{millimeter wavelengths}$) or to

λ [mm]	ν [GHz]	$A_{8000 \text{ km}}$ [μas]	$z = 1$ [mpc]	$z = 0.01$ [mpc]	$r = 10 \text{ kpc}$ [μpc]
6.9	43	90	380	12.9	4.4
3.5	86	45	199	6.4	2.2
1.4	215	18	77	2.6	0.9
0.9	350	11	47	1.6	0.5
linear resolution in [cm]:			10^{17-18}	10^{15-16}	10^{12-13}
in [R_S]:			$10^{3-4} R_S^9$	$10^{2-3} R_S^8$	$10^{1-2} R_S^6$

Table 1. Angular and spatial resolution attainable with ground based mm-VLBI. The table gives the typical observing beam size A (equation (2)) for a 8000 km interferometer baseline (col. 3) depending on wavelength (col. 1) and frequency (col. 2). In columns 4–6 the corresponding spatial scales are given for some typical distances of the objects (using the redshift as distance indicator and $H_0 = 100 \text{ km s}^{-1} \text{ Mpc}^{-1}$, $q_0 = 0.5$). In the lower part of the table the spatial scale is shown in units of [cm] and Schwarzschild-radii [R_S]. With R_S^9 being the Schwarzschild-Radius for a $10^9 M_\odot$ mass black hole, a scale of 1 mpc ($= 3.1 \times 10^{15} \text{ cm}$) corresponds to $\simeq 10 R_S^9$.

place one or more VLBI antennas in space (or on the moon). Efforts in both directions are underway:

Recently fringes with significant signal-to-noise ratios of up to 10 have been detected for the quasars 3C273, 3C279 and 2145+067 at $\lambda = 1.4 \text{ mm}$ ($\nu = 215 \text{ GHz}$) on the 1150 km baseline between the 30 m millimeter radio-telescope at Pico Veleta (near Granada, Spain) and a single antenna of the millimeter radio-interferometer at Plateau de Bure (near Grenoble, France) (Greve *et al.*, 1995). Further VLBI test-experiments at frequencies $\nu \geq 150 \text{ GHz}$ are planned.

In table 1 the angular and spatial resolution, which now or in the near future could be achieved by ground based mm-VLBI is summarized. Depending on the distance to the source, spatial scales of order of $10^2 - 10^4$ Schwarzschild-radii of a $10^9 M_\odot$ mass black hole can be imaged in extragalactic sources. For galactic sources (eg. the Galactic Center Source Sgr A*) regions of 10-100 Schwarzschild-radii (assuming a $10^6 M_\odot$ mass black hole) can be mapped. This is close to the sizes of the expected central accretion disc !

Space VLBI at cm-wavelengths ($\lambda \geq 1.3 \text{ cm}$) with an orbiting VLBI antenna is planned for the very near future (the Japanese satellite ‘VSOP’ will be launched in fall 1996). If successful, this will trigger further technical improvements and future missions. With an open mind for such future developments, it therefore is not unreasonable to assume that on timescales on which also a large sub-millimeter array like the LSA would be completed, space-VLBI observations might be quite common. One therefore should regard mutual observations between earth- and space-based telescopes, even at millimeter wavelengths. Millimeter space-VLBI would yield, for example, an angular resolution of $\sim 4 \mu\text{as}$, if interferometric observations on a 20 000 km baseline are performed at $\lambda = 1 \text{ mm}$

Station Location	Abbrev.	D [m]	T _{sys} [K]	η_A [%]	G _{eff} [K/Jy]
Large Southern Array, type 1	LSA1	50x16	150	0.6	2.16
Large Southern Array, type 2	LSA2	100x11	150	0.6	2.06
NRAO Millimeter Array	MMA	40x 8	150	0.6	0.43
Large Millimeter Telescope, Mexico	LMT	50	150	0.3	0.21
Plateau de Bure, France	Bure	5x15	150	0.3	0.086
Pico Veleta, Spain	Pico	30	150	0.3	0.077
Nobeyama, Japan	NRO	45	150	0.1	0.058
Nobeyama Millimeter Array, Japan	NMA	6x10	150	0.3	0.047
Owens Valley, California	Ovro	6x10.4	150	0.5	0.084
Hat Creek, California	Bima	10x6.1	150	0.5	0.050
Southern European Telesc., Chile	Sest	15	150	0.35	0.022
James Clark Maxwell Telesc., Hawai	JCMT	15	150	0.6	0.038
Kitt Peak, Arizona	KittP	12	150	0.4	0.016
Heinrich Hertz Telescope, Arizona	HHT	10	150	0.6	0.017
Caltech Sub-mm Observatory, Hawai	CSO	10.4	150	0.5	0.015

Table 2. A hypothetical future VLBI-array at $\sim 250 - 300$ GHz. Not all possible participants are listed. Being very optimistic we assumed for each antenna an effective system temperature $T_{\text{sys}} = 150$ K (including atmosphere). The effective antenna gain G_{eff} in [K/Jy] is shown in column 6, and follows from $G_{\text{eff}} \simeq 2.845 \cdot 10^{-4} \cdot \eta_A \cdot D^2$, with the telescope diameter D in [m]. Already existing mm-antennas which are expected to contribute with reduced gain are listed in the lower part of the table.

LSA	LSA/MMA/LMT	3–10 mJy
LSA	Ovro/Bure/Pico/Nobe/Bima/NMA	15–20 mJy
LSA	JCMT/Sest/HHT/KittP/CSO	20–35 mJy
MMA	LMT/Ovro/Bure/Pico/Nobe/Bima/NMA	20–40 mJy
LMT	Bure/Ovro/Pico/Bima/Nobe/NMA	40–60 mJy
	others	$\gtrsim 60$ mJy

Table 3. Typical 7σ VLBI detection thresholds. We assumed 2-bit sampling, 1 GHz bandwidth, 20 sec integration time, and a signal-to-noise ratio of the detection of at least $\text{SNR} \geq 7$. The flux density limits were derived using table 2 and equation (3).

($\nu = 300$ GHz). Even if space-VLBI at the shortest millimeter wavelengths were not feasible by the time the LSA is operating, ground based mm-VLBI observations could complement space-VLBI observations at short cm-wavelengths with their *matching* angular resolution. Thus small scale regions could be imaged with nearly identical resolution at quite different frequencies (eg. 86 GHz space-VLBI and 215 GHz ground-VLBI observations yield similar observing beams).

3 Sensitivity

The single baseline 1σ -detection threshold (in [mJy]) of a VLBI-interferometer consisting of two antennas with diameters D_i and D_j (in [m]), aperture efficiencies η_i and η_j observing with receivers of system temperatures T_{sys}^i and T_{sys}^j (in [K]) at a bandwidth $\Delta\nu$ (in [MHz]) is:

$$\sigma_{ij} = 2.485 \cdot 10^6 \cdot \frac{1}{C_l} \cdot \frac{1}{D_i \cdot D_j} \cdot \sqrt{\frac{T_{\text{sys}}^i}{\eta_i} \cdot \frac{T_{\text{sys}}^j}{\eta_j}} \cdot \frac{1}{\sqrt{\Delta\nu \cdot \Delta t}} \quad (3)$$

where C_l is a VLBI efficiency factor combining quantization and correlator losses (eg. $C_l = 0.88$ for 2-bit sampling), and Δt is the integration time (in [sec]). At mm-wavelengths coherence losses in the atmosphere limit the integration time Δt to a few up to a few tens of a second (note: incoherent averaging of the coherent segments in the initial fringe search allows detection of fringes somewhat beyond the atmospheric coherence time (Rogers *et al.*, 1995)). The limits for single antenna sizes ($D \leq 100$ m), aperture efficiencies ($\eta \lesssim 0.6$), and receiver performances ($T_{\text{RX}} \gtrsim 50 - 100$ K for $\nu \geq 50$ GHz) do not allow a substantial lowering of the detection threshold. Some improvement could be obtained from the extension of the observing bandwidth, but a major step could only be done with an increase of the effective collecting area.

The MK IV and VLBA data acquisition systems will provide data recording with extended bandwidths of up to $\Delta\nu = 512$ MHz in the foreseeable future. But even if observations with GHz-bandwidth were possible (and if the problems of phasing an array at such a large bandwidth are solved), the VLBI-detection limit can be pushed by not much more than a factor of ~ 3 .

A large collecting area of order of 10^4 m² requires an aperture synthesis instrument. The addition of such a phased array to an existing network of smaller VLBI-telescopes would lower the VLBI-detection threshold at millimeter wavelengths drastically. As illustrating example, we list the station performances of a hypothetical future mm-VLBI array in table 2. We included both suggested configurations for the LSA (50×16 m antennas (LSA1) or 100×11 m antennas (LSA2)) and assumed also that the proposed NRAO Millimeter Array (MMA) and the UMASS/INAOE Large Millimeter Telescope (LMT) will be operating. From equation (2) and with some simplifying assumptions on antenna and receiver characteristics, we estimated the VLBI-detection limits, which we summarize in table 3. It is obvious that the combination of the LSA with other large sub-mm telescopes pushes the detection threshold towards the 5 – 10 mJy level. More optimistic assumptions on observing bandwidth and receiver performances would even lower these sensitivity limits.

The addition of one very sensitive antenna to a VLB-array consisting mainly of smaller antennas produces a considerable improvement of the dynamic range of the images (see eg. C. Walker, 1989):

$$\frac{1}{\Delta S^2} = \sum_{i,j}^{\text{all baselines}} \frac{1}{\sigma_{ij}^2} \quad (4)$$

where ΔS (in [mJy]) is the noise in the map, σ_{ij} is taken from equation (3), and the sum is over all $N(N-1)/2$ baseline combinations of the interferometer array. Replacing for example one antenna in an array of 5 equal 30 m antennas by the phased LSA would cause a reduction in the map noise by a factor of 3 to about $\sigma = 1$ mJy. This and the fact that the single baseline ‘a-priori’ detection threshold between two smaller and less sensitive antennas can be reduced, if ‘fringes’ to a third more sensitive antenna are detected (the method of ‘global fringe fitting’ uses the closure relations in such antenna triangles, eg. Schwab & Cotton, 1983, Alef & Porcas, 1986), emphasizes the dramatical improvement of the data quality, which could be achieved, if the LSA is added to any preexisting VLB-array.

4 What can be observed ?

From equation (1) and (2) the lowest detectable brightness temperature can be written as:

$$T_B[\text{K}] \geq 1.27 \cdot \Delta S_{[\text{mJy}]} \cdot b_{[\text{km}]}^2 \cdot r^{-2} \quad (5)$$

where the ratio r of source size to the interferometer beam ($r = \theta_{\text{source}}/A$) measures the source extent, b the maximum baseline length of the interferometer and ΔS the noise level in the map (equation (4)). With a detection limit of $\Delta S \simeq 1$ mJy and source sizes in the range $0 \leq r \leq 10$, the lowest detectable brightness temperature at $\nu = 300$ GHz is $T_B \geq 10^{2-4}$ K for a 100 km baseline ($A = 1$ mas), $T_B \geq 10^{4-6}$ K for a 1000 km baseline ($A = 0.1$ mas) and $T_B \geq 10^{6-8}$ K for a 10000 km baseline ($A = 0.01$ mas). In figure 1 this result is also displayed graphically.

Thus it is clear that most compact nonthermal radio sources and the brighter thermal objects ($T_B \gtrsim 10^{5-6}$ K) are accessible for mm-VLBI including the LSA. It can be expected that such observations substantially would improve our understanding of the various forms of nuclear activity in galaxies (eg. starbursts, mergers, central black holes) and quasars (accretion, production and propagation of jets, particle acceleration processes). High dynamic range mm-VLBI-imaging with micro-arcsecond resolution will reveal more insight in the central light-day size regions of these objects, self-absorbed at longer wavelengths. This should result in a much more detailed understanding of the still unsolved problem of energy production in active galactic nuclei (AGN).

VLBI imaging of high redshift quasars ($z \geq 3$) and gravitational lenses at mm-wavelengths can help in answering questions on the metric and structure of our universe. The extension of the angular size-distance relation towards smaller source sizes and larger distances, could help to more accurately determine the cosmological deceleration parameter q_0 (eg. Kellerman *et al.*, 1993, Gurvits *et al.*, 1994) or even the cosmological constant Λ (Krauss & Schramm, 1993).

With its inverted radio spectrum ($\alpha > 0$, $S_\nu \propto \nu^\alpha$), the flux density of thermally emitting objects increase from the cm- to the mm-regime. With a planned maximum antenna spacing of $\lesssim 10$ km and an angular resolution of $\gtrsim 10$

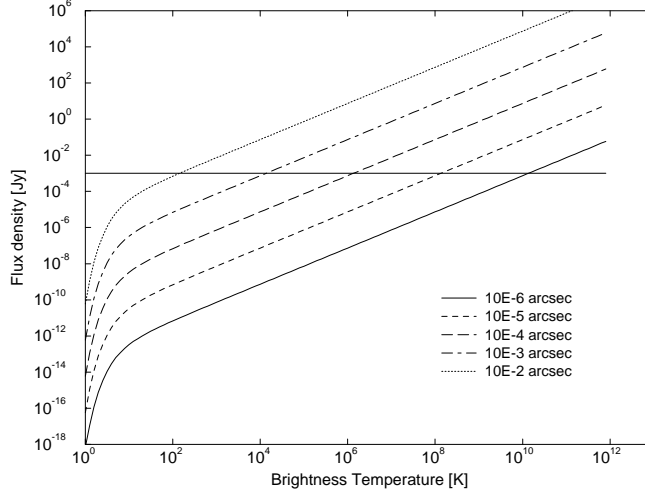


Fig. 1. Flux density of a Planck-black-body radiator plotted versus brightness temperature. The curves are for different source sizes ranging from $1\mu\text{as}$ (10^{-6} arcsec, lower solid line) to 10 mas (10^{-2} arcsec, upper dotted line). The horizontal line gives a hypothetical VLBI detection threshold of $S_{\text{min}} = 1\text{ mJy}$. For a given source size, the minimum detectable brightness temperature can be found at the position where horizontal line and radiation curve intersect.

mas, the LSA will be particularly useful for detailed studies of low brightness temperature objects $T_B \lesssim 100\text{ K}$. At the mJy-level, radio stars with brightness temperatures in the range of $T_B = 10^{3-5}\text{ K}$ have sizes in the milli-arcsecond range (see Altenhoff *et al.*, 1994 for more details on radio stars). Thus studies of stars, stellar winds or even stellar surfaces would become possible, if the LSA and other sensitive antennas (eg. MMA, LMT) were used as a long baseline interferometer covering only intermediate baseline lengths in the range of typically $10 - 1000\text{ km}$. In the radio cm-bands the thermal part of the spectrum of a radio source (eg. a radio star) is too faint to be observable with VLBI. In the mm-bands this part may reach flux densities of order of up to a few mJy and sizes of less than a few or a few ten milli-arcseconds. Millimeter-VLBI observations with the LSA and possibly the MMA and other large antennas will for the first time allow direct imaging of such objects.

5 Summary

The planned large southern array will dramatically improve the quality of scientific research at millimeter wavelengths. With its large collecting area it could play an important role in future mm-VLBI observations, pushing the sensitivity to the milli-Jansky level. In VLBI, such high sensitivity at present is achieved only at the longer cm-wavelengths. Since thermal radiation becomes more dominant towards shorter wavelengths, mm-VLBI with milli-Jansky sensitivity will not only allow imaging of compact non-thermal radio sources, but also mapping of thermally emitting objects like stars or hot compact regions in extragalactic objects. With an angular resolution of micro-arcseconds, high sensitivity mm-VLBI or even space mm-VLBI (using an orbiting mm-antenna) will allow imaging of regions not directly accessible by any other method. It is therefore not unreasonable to assume that this observing method could yield spectacular scientific results, improving our present knowledge of many astronomical objects in the universe.

Acknowledgements: VLBI observations at millimeter wavelengths are a joint effort of numerous people, impossible to list here. We wish to express thanks to all of them. The following observatories were involved in recent 86 GHz VLBI campaigns: MPIfR (100 m Telescope), IRAM (Pico Veleta, Plateau de Bure), NRAO (Kitt Peak), Onsala, Sest, Haystack, Quabbin, the Owens Valley Caltech interferometer (OVRO), and the Berkeley Hat Creek interferometer (BIMA). The author appreciates financial support from the German BMFT-Verbundforschung.

References

- Alef, W. & Porcas, R., 1986, *A&A*, **168**, 365.
- Altenhoff, W.J., et al., 1994, *A&A*, **281**, 161.
- Bååth, L.B., et al., 1992, *A&A*, **257**, 31.
- Gurvits, L.I., et al., 1994, *ApJ*, **425**, 442.
- Greve, A., et al., 1995, *A&A*, **299**, L33.
- Kellermann, K.I., 1993, *Nat*, **361**, 123.
- Krauss, L.M., & Schramm, D.N., 1993, *ApJ*, **405**, L43.
- Krichbaum, T.P., et al., 1993, *A&A*, **275**, 375.
- Krichbaum, T.P., et al., 1994, in: *Compact Extragalactic Radio Sources*, ed. J.A. Zensus and K.I. Kellermann (NRAO, Socorro), p. 39.
- Padin, S., et al., 1990, *ApJ*, **360**, L11.
- Rogers, A.E.E., et al., 1984, *Radio Science*, **19**, 1552.
- Rogers, A.E.E., et al., 1995, *AJ*, **109**, 1391.
- Schalinski, C.J., et al., 1994, in: *Compact Extragalactic Radio Sources*, ed. J.A. Zensus and K.I. Kellermann (NRAO, Socorro), p. 45.
- Schwab, F.R., & Cotton, W.D., 1983, *AJ*, **88**, 688.
- Standke, K.S., et al., 1994, in: *VLBI Technology, Progress and Future Observational Possibilities*, ed. T. Sasao, S. Manabe, O. Kameya, and M. Inoue (Terra Scientific Publishing Company, Tokyo), p. 86.

- Thompson, A.R., Moran, J.M., and Swenson, G.W. (eds.), *Interferometry and Synthesis in Radio Astronomy*, (Wiley & Sons: New York), 1986.
- Wagner, S.J., & Witzel, A., 1995, *ARA&A*, **33**, 163.
- Walker, C., 1989, in: *Very Long Baseline Interferometry, Techniques and Applications*, eds. M. Felli & R.E. Spencer, Nato ASI Series Vol. 283 (Kluwer: Dordrecht), p. 163.
- Zensus, J.A, Diamond, P.J., and Napier, P.J., (eds.), *Very Long Baseline Interferometry and the VLBA*, ASP Conference Series, Vol. 82, 1995.